Ling, Chen; Nguejio, Josiane; Manno, Riccardo; St-Pierre, Luc; Barbe, Fabrice; Benedetti, Ivano

Fracture of Honeycombs Produced by Additive Manufacturing

Published in:
Journal of Multiscale Modelling

DOI:
10.1142/S1756973721440066

Published: 01/06/2022

Document Version
Peer-reviewed accepted author manuscript, also known as Final accepted manuscript or Post-print

Please cite the original version:
Ling, C., Nguejio, J., Manno, R., St-Pierre, L., Barbe, F., & Benedetti, I. (2022). Fracture of Honeycombs Produced by Additive Manufacturing. *Journal of Multiscale Modelling*, *13*(2), Article 2144006. https://doi.org/10.1142/S1756973721440066

Journal of Multiscale Modelling

Fracture of honeycombs produced by additive manufacturing

Chen Ling

Department of Mechanical Engineering, Aalto University
*Espoo 02150, Finland.**

Josiane Nguejio

Normandie University, INSA Rouen, UNIROUEN, CNRS, GPM, UMR 6634
76000 Rouen, France.

Riccardo Manno

Bristol Composite Institute (ACCIS), Department of Aerospace Engineering,Queen's Building,
University Walk
Bristol, BS8 1TR, United Kingdom.

Luc St-Pierre

Department of Mechanical Engineering, Aalto University,
Espoo 02150, Finland.

Fabrice Barbe

Normandie University, INSA Rouen, UNIROUEN, CNRS, GPM, UMR 6634
76000 Rouen, France.

Ivano Benedetti

Department of Engineering, University of Palermo, Viale delle Scienze, Edificio 8
90128, Palermo, Italy.

Received January 19, 2022
Revised (Day Month Year)

Lattice materials, such as honeycombs, are remarkable in their ability to combine high stiffness, strength and toughness at low density. In addition, the recent and pervasive development of additive manufacturing technologies makes it easier to produce these cellular materials and opens new possibilities to improve their properties by implementing small modifications to their microstructure. This study aims is to show that the work of fracture of honeycombs can be increased with density variations. To achieve this, single-edge notched tension specimens, with a honeycomb lattice structures, were manufactured by stereolithography using a ductile polymer resin. The performances of three different honeycombs were compared: *(i)* a uniform sparse lattice, *(ii)* a uniform dense lattice, and *(iii)* a gradient lattice with alternating bands of sparse and dense lattices. The

*Corresponding author: chen.1.ling@aalto.fi

results indicated that specimens with a density gradient may achieve a normalised work of fracture up to 146% higher than that of a uniform lattice.

Keywords: 3D printed lattices; Bio-inspired materials; Fracture mechanics.

1. Introduction

Lattice materials, in the form of foams[1] or micro-architectured materials[2], possess a unique combination of low density and high relative mechanical performances. For this reason, lattices are considered key enablers for the next generation of aerospace and automotive technologies. Indeed, the production of structural components with a lower weight and able to deliver the same mechanical performances allows reducing fuel consumption and consequently, lowers the application environmental footprint. Furthermore, lattice materials offer an interesting set of other properties such as: *(i)* high energy absorption per unit mass *(ii)* mechanical damping *(iii)* low acoustic and thermal conductivity and *(iv)* tunable porosity.

Even though the properties of lattices are highly appealing, their deployment in primary structural applications has been hindered by a certain scatter in their mechanical response[3], which stems from a lack of control of their microstructural features, even when additive manufacturing (AM) is employed. Indeed, as shown by Ramezani *et al.*[4], the printing direction may have a significant influence on the overall mechanical response of the lattice material. However, the continuous development of AM technologies is rapidly improving the level of control on the material microstructure and the resolution of the manufactured components[5], offering promising perspectives for the materials by design paradigm.

The improvements in AM technologies offer unprecedented opportunities to fill voids in the design space as they allow creating microstructural patterns of lattice struts to achieve specific properties. While some researchers seek through the innumerable possible configurations using structural optimisation tools[6], others focus on the invaluable inspiration given by nature. Nature provides numerous examples of materials characterised by outstanding properties thanks to an optimised hierarchical multi-scale arrangement of elementary constituents[7]. For example, several kinds of woods have density variations that are associated with a tougher mechanical response, and the numerical simulations of Manno *et al.*[8] showed that honeycombs with similar density variations have a work of fracture up to 50% higher than their uniform counterparts. This study extends the work performed in Manno *et al.*[8,9] by complementing it with experimental tests performed on three types of honeycombs produced by AM using stereolithography.

The fracture toughness of regular honeycombs has been investigated analytically[10], numerically[11,12] and experimentally[13]. These studies found that the cell walls of a honeycomb fracture in bending and that the fracture toughness K_{Ic} scales with the volume fraction of material $\bar{\rho}$ as $K_{Ic} \propto \bar{\rho}^2$ and with the cell size ℓ as $K_{Ic} \propto \sqrt{\ell}$. These scaling laws, initially obtained for an elastic-brittle parent material, were also found to be valid for honeycombs made from an elastic-plastic

material[14]. Recently, simulations by Hsieh *et al.*[15] indicated that honeycombs have a flat R-curve and therefore, a relatively low resistance to crack propagation. In this study, we aim to increase the resistance to crack propagation by designing honeycombs with variations in density.

This article is structured as follows. The design and manufacture of honeycombs with and without density variations are described in Section 2. Then, the results of single-edge notch tensile tests are presented in Section 3 and the work of fracture is used to assess the effectiveness of density variations.

2. Materials and methods

Single-edge notch specimens, with a hexagonal lattice structure, were manufactured with the dimensions shown in Fig. 1. Three types of samples were considered: *(i)* a gradient lattice, where bands of sparse and dense hexagonal cells are alternated, see Fig. 1; *(ii)* a uniform lattice made of sparse hexagonal cells only; and *(iii)* a uniform lattice made of dense hexagonal cells only. These three types of samples had the same overall dimensions and initial notch length.

In the gradient specimens, the proportion of sparse cells with respect to dense ones was selected based on the numerical analyses of Manno *et al.*[8], which aimed to maximise the work of fracture. The design of the specimens and the choice of the cell dimensions were similar to those previously manufactured in Manno *et al.*[9], allowing a comparison between two different materials and printing techniques (a polymeric resin produced by stereolitography here versus a thermoplastic, ABS, elaborated by fused filament fabrication in Manno *et al.*[9]). In contrast with the previous ABS specimens, a small modification to the design has been made: the

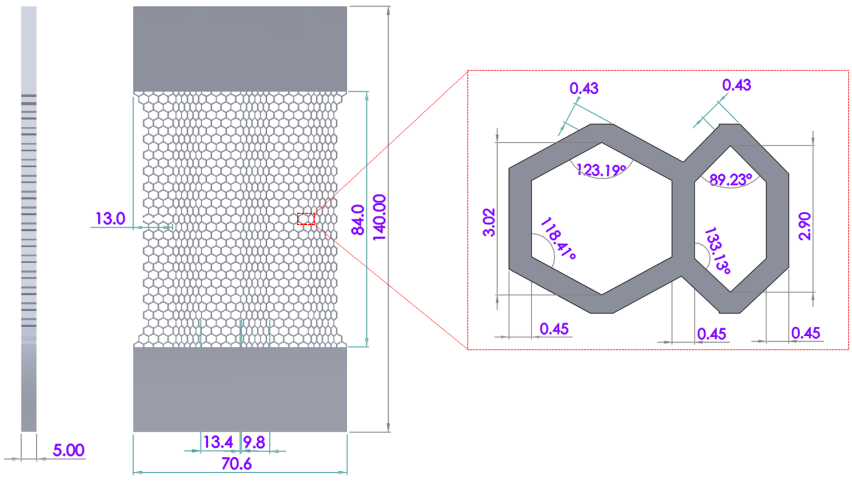

Fig. 1. Dimensions of a single-edge notch tension specimen with a density gradient lattice. All dimensions are in mm.

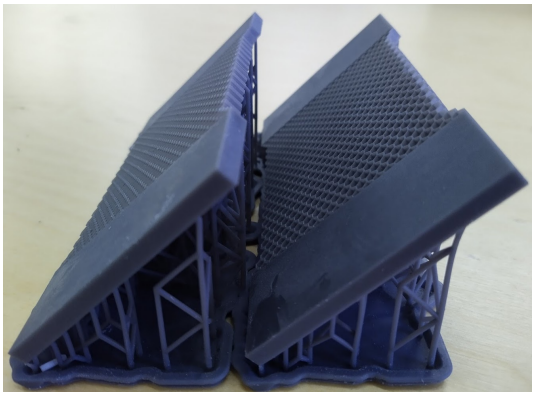

Fig. 2. Photograph of two samples printed at 45°, after curing and before removing the supports.

width of the lattice is slightly narrower than the width of the gripping areas, see Fig. 1. This was necessary to avoid fracture close to the grips (note, however, that this was not needed in previous tests on ABS samples as they failed at much lower strains).

All samples considered in the present study were fabricated by stereolithography using a Form 3 machine from Formlabs[16]. The parent material was a ductile polymeric resin called Tough 2000 and also provided by Formlabs. All specimens were printed with a 50 μm layer resolution and orientated at 45° from the printing bed, see Fig. 2. After printing, each sample was cured at 70°C in the Form Cure oven for 60 min in accordance with Formlabs recommendation. The specimen was then separated from its supports and kept at room temperature for five hours before testing. Finally, all samples were loaded in tension using a standard mechanical testing machine (Zwick Z020) with a displacement rate of 2 mm/min.

Standard dog-bone specimens were also manufactured, following the procedure detailed above, to measure the tensile response of the Tough 2000 resin, which is shown in Fig. 3. The resin has a Young's modulus of 0.65 GPa up to a yield strength of about 37.3 MPa. The three stress-strain curves show a good repeatability, but the failure strain displays more variability ranging from 0.4 to 0.5.

3. Results

The measured force-displacement responses are shown in Fig. 4, where the three types of specimens are compared. All responses have a linear elastic regime, followed by non-linear deformation up to the peak force. Subsequently, the load drops as the crack propagates from the notch, and this softening response is more abrupt for the gradient lattice compared to uniform samples (sparse and dense). Each geometry was tested twice and the results display a good repeatability, with very similar responses up to the peak force.

Photographs were taken during the tests to capture the crack propagation paths,

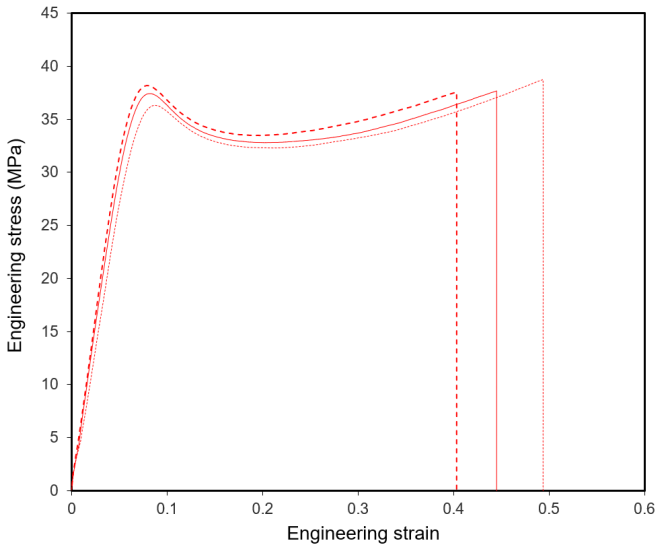

Fig. 3. Tensile response of the Tough 2000 resin measured on three standard dog-bone specimens produced using the same AM process as that employed for the hexagonal lattice structures.

and these are presented in Fig. 5 for each type of lattices. In all cases, the crack propagated from the initial notch and grew following a path approximately straight, although an initial clear deflection is always highlighted at the first interface between a sparse and a dense band. The crack front remained within the gauge length of the specimen and, as expected from the novel specimen design, no wall failure was observed close to the gripping areas. The crack propagated in a relatively steady manner for uniform lattices (sparse and dense), which lead to a progressive softening in their force-displacement responses, see Fig. 4. In contrast, the crack grew in steps through the gradient lattice: the crack propagated from the initial notch and stopped at the next band of dense hexagonal cells, see Fig. 5. This process explains the step-wise tensile response for the gradient lattice in Fig. 4 and it is consistent with the the observations on ABS specimens[9].

The work of fracture W, defined as the area under the force-displacement response, was evaluated for each specimen and the results are given in Table 1. The three types of samples have a different relative density $\bar{\rho}$ (defined as the density of the honeycomb structure divided by the density of the parent material), and therefore, the normalised work of fracture $W/\bar{\rho}$ is given in Table 1 to allow a fair comparison. The gradient lattice has the highest normalised work of fracture; it is 66 to 146% higher than that of the sparse lattice and 3 to 29% higher than that of the dense lattice, see Table 1. The performance increase with respect to the dense lattice, although seemingly limited, signals the possibility of saving material without compromising and even enhancing toughness of structural components. The mechanism explaining this increase in performances is presumably the mismatch in

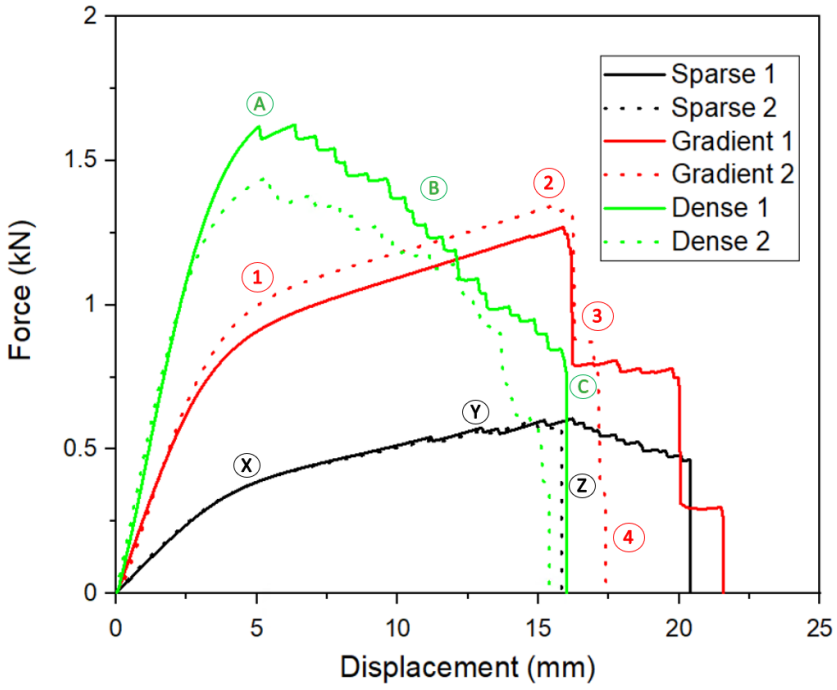

Fig. 4. Tensile responses for the three types of lattice structures. The labels inside circular symbols refer to the photographs presented in Fig. 5.

fracture toughness between the dense and sparse bands, as elucidated by the numerical analyses of Manno *et al.*[8]. These interfaces not only act as crack arrestors (increasing the energy necessary for further propagation), but also produce two separate equally intense stress concentration zones ahead of the notch tip instead of one, which leads to crack kinking as observed in numerical simulations and on ABS specimens, see Fig. 6.

The experimental results reported above are encouraging evidence for the effectiveness of density gradient honeycombs. In this study, the dense bands were created by reducing the width of the hexagonal cells, see Fig. 1 (instead of keeping the cell size fixed and increasing the thickness of the cell walls). This could introduce size effects as the ratio of the initial notch length divided by the cell size is greater for the dense lattice compared to the sparse honeycomb. We anticipate that this would not affect the above conclusions since increasing the cell size ℓ in the dense bands will increase the fracture toughness K_{Ic} of both dense and gradient honeycombs with respect to the sparse design (recall that $K_{Ic} \propto \sqrt{\ell}$). Nonetheless, numerical work is underway to quantify this size effect.

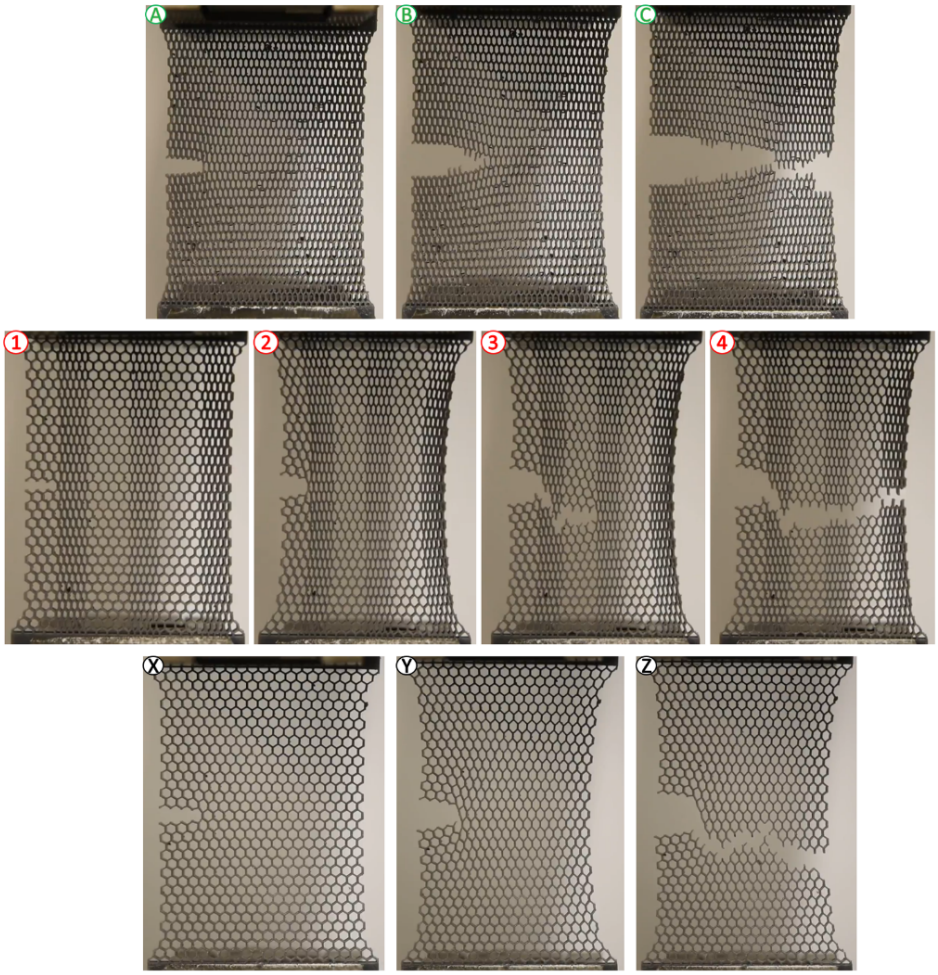

Fig. 5. Photographs showing the crack path for dense (top row), gradient (middle row) and sparse (bottom row) lattice structures.

4. Conclusions

In this study, we used stereolithography to manufacture single-edge notched tension specimens with hexagonal lattice structures and we investigated their fracture behaviour under tensile loading. The performances of three different designs were compared: *(i)* a uniform sparse lattice, *(ii)* a uniform dense lattice, and *(iii)* a gradient design made from alternating sparse and dense lattice layers. The experiments presented good repeatability and demonstrated the effectiveness of the density gradient concept: the normalised work of fracture for the gradient design was up to 146% higher than that of the sparse lattice and 29% higher than that of the dense

Table 1. Comparison between the fracture performances of each sample.

Sample	Work of fracture W (J)	Relative density $\bar{\rho}$	$W/\bar{\rho}$ (J)
Sparse 1	9.05	0.27	33.5
Sparse 2	6.60		24.4
Gradient 1	18.62	0.31	60.1
Gradient 2	17.24		55.6
Dense 1	18.87	0.35	53.9
Dense 2	16.30		46.6

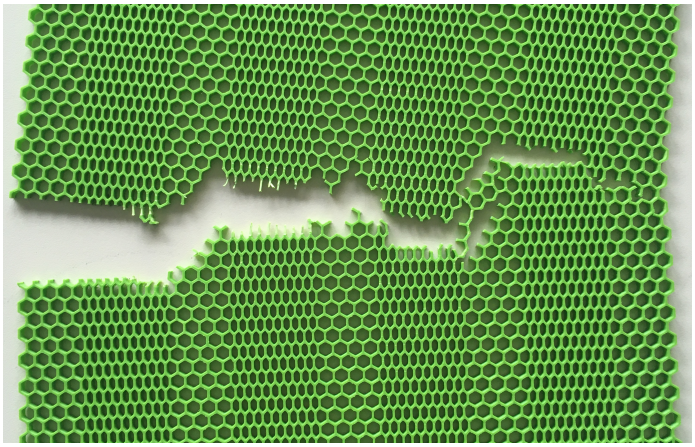

Fig. 6. Photograph showing the crack path in a gradient honeycomb made of ABS, from Ref. 9.

lattice. These preliminary results are encouraging and contributing to current efforts in developing high toughness lattice materials[17]. Further work is underway to vary the arrangement and proportions of sparse and dense layers with the objective of maximising the work of fracture in density gradient lattices. Applications will concern both ABS lattices manufactured from fused filaments and resin lattices manufactured using stereolithography. These parent materials will provide a large span of tensile properties to evaluate the ability of numerical modelling to quantitatively predict fracture energies.

Acknowledgments

CL acknowledges the support from ADDLAB for manufacturing the samples and the assistance of Kim Widell for conducting the experiments. CL and LS are grateful for the financial support provided by the Academy of Finland (decision 322007). JN and FB acknowledge the Region Normandy of France for its financial support as part of the project RIN Recherche PFAN-1.

References

1. J. Banhart, *Mater. Sci.* **46** 559 (2001).
2. M. Rashed, M. Ashraf, R. Mines, and P. J. Hazell, *Mater. Des.* **95** 518 (2016).
3. U. Ramamurty and A. Paul, *Acta Mater.* **52** 869 (2004).
4. H. Ramezani Dana, F. Barbe, L. Delbreilh, M. B. Azzouna, A. Guillet, and T. Breteau, *J. Manuf. Process.* **44** 288 (2019).
5. T. Frenzel, M. Kadic, and M. Wegener, *Science* **358** 1072 (2017).
6. J. Robbins, S. Owen, B. Clark, and T. Voth, *Addit. Manuf.* **12** 296 (2016).
7. M. Meyers and P. Chen, *Biological Materials Science: Biological Materials, Bioinspired Materials, and Biomaterials* (Cambridge University Press, 2014).
8. R. Manno, W. Gao, and I. Benedetti, *Extreme Mech. Lett.* **26** 8 (2019).
9. R. Manno, J. Nguejio, F. Barbe, and I. Benedetti, *AIP Conference Proceedings* **2309** 020015 (2020).
10. L. J. Gibson and M. F. Ashby, *Cellular solids: structure and properties* (Cambridge University Press, 1997).
11. J. S. Huang and L. J. Gibson, *Acta Metall. Mater.* **39** 1617 (1991).
12. N. A. Fleck and X. Qiu, *J. Mech. Phys. Solids* **55** 562 (2007).
13. P. E. Seiler, H. C. Tankasala, and N. A. Fleck, *Acta Mater.* **171** 190 (2019).
14. H. C. Tankasala, V. S. Deshpande, and N. A. Fleck, *J. Appl. Mech.* **82** 91004 (2015).
15. M.-T. Hsieh, V. S. Deshpande, and L. Valdevit, *J. Mech. Phys. Solids* **138** 103925 (2020).
16. Formlabs, Somerville (MA) USA, https://formlabs.com, accessed: 2021-12-04.
17. Y. Liu, L. St-Pierre, N. A. Fleck, V. S. Deshpande, and A. Srivastava. *J. Mech. Phys. Solids* **143** 104060 (2020).